Published in final edited form as:
Circ Res. 2009 January 2; 104(1): 79–86. doi:10.1161/CIRCRESAHA.108.183475.

Oxidative Stress-Induced Afterdepolarizations and Calmodulin Kinase II Signaling

Lai-Hua Xie[2], **Fuhua Chen**[1], **Hrayr S. Karagueuzian**[1], and **James N. Weiss**[1]

[1]Cardiovascular Research Laboratory, David Geffen School of Medicine, University of California, Los Angeles, California 90095

[2]Department of Cell Biology and Molecular Medicine, UMDNJ-New Jersey Medical School, Newark, NJ 07101

Abstract

In the heart, oxidative stress caused by exogenous H_2O_2 has been shown to induce early afterdepolarizations (EADs) and triggered activity by impairing Na current (I_{Na}) inactivation. Since H_2O_2 activates Ca^{2+}/calmodulin kinase II (CaMKII), which also impairs I_{Na} inactivation and promotes EADs, we hypothesized that CaMKII activation may be an important factor in EADs caused by oxidative stress. Using the patch clamp and intracellular Ca (Ca_i) imaging in Fluo-4 AM-loaded rabbit ventricular myocytes, we found that exposure to H_2O_2 (0.2–1mM) for 5-15 min consistently induced EADs that were suppressed by the I_{Na} blocker tetrodoxtin (TTX, 10 μM), as well as the $I_{Ca,L}$ blocker nifedipine. H_2O_2 enhanced both peak and late $I_{Ca,L}$, consistent with CaMKII-mediated facilitation. By prolonging the AP plateau and increasing Ca influx via $I_{Ca,L}$, H_2O_2-induced EADs were also frequently followed by DADs in response to spontaneous (i.e. non $I_{Ca,L}$-gated) SR Ca release after repolarization. The CaMKII inhibitor KN-93 (1 μM, n=4), but not its inactive analog KN-92 (1 μM, n=5), prevented H_2O_2-induced EADs and DADs, and the selective CaMKII peptide inhibitor AIP (2 μM) significantly delayed their onset. In conclusion, H_2O_2-induced afterdepolarizations depend on both impaired I_{Na} inactivation to reduce repolarization reserve, and enhancement of $I_{Ca,L}$ to reverse repolarization, both facilitated by CaMKII activation. Our observations support a link between increased oxidative stress, CaMKII activation and afterdepolarizations as triggers of lethal ventricular arrhythmias in diseased hearts.

Keywords

Reactive oxidative species; early afterdepolarization; triggered activity; arrhythmia; CaM Kinase

Introduction

Reactive oxygen species (ROS) are generated as natural byproducts of normal oxygen metabolism and play important roles in cell signaling. However, under pathological conditions, such as heart failure and ischemia-reperfusion, ROS levels can become elevated and predispose the heart to arrhythmias[1 2]. Oxidative stress induced by exposure to hydrogen peroxide (H_2O_2) and other agents has been shown to induce early afterdepolarizations (EADs), delayed afterdepolarizations (DADs) and triggered activity (TA), [3-6], primarily attributed in previous studies to impaired inactivation of Na current (late I_{Na}) [4, 5]. However, H_2O_2 also affects other

Correspondence to: James N. Weiss, MD, Division of Cardiology, Rm 3645 MRL Building, UCLA, School of Medicine, Los Angeles, CA 90095. jweiss@mednet.ucla.edu.

Disclosures: None.

ion channel and transporters, including the L-type Ca current ($I_{Ca,L}$) [7-9], K currents [10], ryanodine receptors (RyR) [11, 12], sarcoplasmic reticulum (SR) Ca pump SERCA2a [13], and the Na-Ca exchanger (I_{NCX}) [14, 15], which also may influence EADs and TA.

Recently, H_2O_2 has been shown to activate Ca/calmodulin (CaM) kinase II (CaMKII) in cardiac myocytes and other cells [16-18], by direct oxidation of paired Met residues (Met281/282) in the regulatory domain. It is notable that binding of Ca^{2+}/CaM is required to expose the redox sites in the regulatory domain in order for oxidation to persistently activate CaMKII [18]. In addition, ventricular myocytes isolated from transgenic mice overexpressing CaMKIV have been shown to exhibit EADs and TA. Increased endogenous CaMKII activity accompanied EADs and VT/VF observed during telemetry in this mouse model[19]. Alterations in I_{CaL} properties have been implicated as a major factor by which CaMKII activation promotes EADs [19, 20], but a recent study demonstrated that CaMKII activation also increases the late I_{Na} 21, similar to H_2O_2. CaMKII inhibition has been shown to suppress EADs and triggered activity. In a genetic heart failure model, for example, CaMKII inhibition prevented EADs, triggered activity and improved mortality[19]. The ability of pharmacologic agents such as clofilium to induce EADs in isolated rabbit ventricular myocytes [22] was also suppressed by CaMKII inhibition.

Taken together, this evidence led us to hypothesize that activation of CaMKII by oxidative stress may be an important factor in arrhythmogenic effects of H_2O_2. Accordingly, we used isolated patch-clamped rabbit ventricular myocytes and Ca_i imaging to analyze the ionic mechanism(s) underlying H_2O_2-induced afterdepolarizations in the absence and presence of CaMKII inhibition. Our findings support a direct link between oxidative stress, CaMKII activation and the genesis of TA due to afterdepolarizations.

Methods

Cell isolation

Ventricular myocytes were enzymatically isolated from adult rabbit hearts. Briefly, hearts were removed from adult New Zealand white rabbits (2-3 kg) anesthetized with intravenous pentobarbital, and perfused retrogradely in Langendorff fashion at 37°C with nominally Ca-free Tyrode's solution containing ~1.4 mg/ml collagenase (Type II; Worthington) and 0.1 mg/ml protease (type XIV, Sigma) for 25-30 minutes. After washing out the enzyme solution, the hearts were removed from the perfusion apparatus, and swirled in a culture dish. The Ca concentration was slowly increased to 1.8 mM and the cells were stored at room temperature and used within 8 hours.

Intracellular Ca measuremen

Myocytes were loaded with the Ca indicator Fluo-4 by incubating them for ~30 minutes in bath solution containing 4 μM Fluo-4 AM (Molecular Probes) and 0.016% (wt/wt) pluronic (Molecular Probes), after which the cells were washed and placed in a heated chamber on an inverted microscope. Ca_i fluorescence was recorded using an Andor Ixon Charge Coupled Device (CCD) camera (Andor Technology) operating at ~100 frames per second with a spatial resolution of 512 × 180 pixels. The fluorescence intensity was recorded in arbitrary units.

Patch Clamp Methods

Myocytes were patch-clamped using the whole-cell configuration of the patch clamp technique. For AP recordings, patch pipettes (resistance 2–4 MΩ) were filled with pipette solution containing (in mM): 110 K-Aspartate, 30 KCl, 5 NaCl, 10 HEPES, 0.1 EGTA, 5 MgATP, 5 creatine phosphate, 0.05 cAMP, pH 7.2 with KOH. In some experiments, the CaMKII inhibitor peptide AIP (2-10 μM) (Biomol, or Sigma) was added directly to the pipette

solution. The cells were superfused with standard Tyrode's solution containing (in mM): 136 NaCl, 5.4 KCl, 0.33 Na_2PO_4, 1.8 $CaCl_2$, 1 $MgCl_2$, 10 glucose and 10 HEPES, pH 7.4 adjusted with NaOH. To isolate $I_{Ca,L}$, patch pipettes (resistance 2–4 MΩ) were filled with pipette solution containing (in mM): 110 Cs-Aspartate, 30 CsCl, 5 NaCl, 10 HEPES, 0.1 EGTA, 5 MgATP, 5 creatine phosphate, 0.05 cAMP, pH 7.2 with KOH, and the cells were superperfused with a modified Tyrode's solution in which KCl was replaced by CsCl. H_2O_2 (0.2-1 mM) was added directly to the bath superfusate. Nifedipine (Sigma), KN-93 and KN-92 (Biomol) were dissolved in dimethyl sulfoxide (DMSO) as stock solution before diluting into the superfusate solution at the final concentration. The maximum DMSO concentration was <1/500 (v/v). Chemicals and reagents were purchased from Sigma unless indicated. Voltage or current signals were measured with an Axopatch 200B patch-clamp amplifier controlled by a personal computer using a Digidata 1200 acquisition board driven by pCLAMP 8.0 software (Axon Instruments, Foster City, CA). Action potentials were elicited with 2 ms, 2-4 nA square pulses at pacing cycle lengths (PCL) of 6 sec.

All experiments were performed at 34-36°C. Data are presented as mean ± SEM. Statistical significance was assessed using unpaired Student's t-tests, with $p < 0.05$ considered significant.

Results

H_2O_2-induced EADs and DADs in adult rabbit ventricular myocytes

APs were recorded from isolated rabbit ventricular myocytes using whole-cell current clamp mode. After AP duration (APD) and morphology reached steady state, cells were superfused with 0.2-1 mM H_2O_2. The generation of EADs by H_2O_2 was highly dependent on the pacing cycle length (PCL). Typically, at long PCLs (e.g. 6 sec), EADs occurred with every AP, and at short PCL (e.g. 1 s), no EADs occurred. In the intermediate range, EADs occurred irregularly. Therefore, to elicit EADs most reliably, we used a PCL of 6 sec throughout. EADs appeared after an average exposure time of 6.9 ± 1.1 min with 0.2 mM H_2O_2 (n=10), and 6.6 ± 0.8 min with 1 mM H_2O_2 (n=12). As shown in Fig. 1A, EADs could be irregular, single or multiple with an oscillating membrane potential before repolarization (Fig. 1 A & B). DADs were also observed after prolonged perfusion of H_2O_2 and occasionally triggered APs (Fig 1B, right panel). DADs often occurred following a previous AP with an EAD (Fig. 1B middle panel and 1C), presumably because the prolonged APD allowed maintained $I_{Ca,L}$ to overload the SR with Ca. Prolonged perfusion (15-20 min) of H_2O_2 eventually caused gradual depolarization of the resting membrane potential to less than -40 mV and the cells became inexcitable.

Ionic mechanisms of H_2O_2-induced EADs and DADs

We next used pharmacologic interventions to analyze the ionic and cellular mechanism(s) underlying H_2O_2-induced aftedepolarizations. As shown in Fig. 2A, H_2O_2-induced EADs were reversibly suppressed by the selective Na current blocker TTX (10 μM), which also shortened APD. Ranolazine (20 μM), a more selective blocker of late I_{Na}, also eliminated H_2O_2-incuded EADs and shortened APD (data not shown), consistent with previous reports by Song et al [4, 5] implicating late I_{Na} as playing a key role. Unlike H_2O_2, anemone toxin II (ATX), an agent that selectively delays the late phase inactivation of I_{Na} 23, failed to induce frank EADs, producing instead only small (1-2 mV) irregular oscillations during phase 2 of the AP. Note that APD was prolonged by ATX to a greater extent than after H_2O_2 (Fig. 2B), yet no EADs were observed. This finding indicates that activation of late I_{Na} is not, by itself, sufficient to produce EADs under these experimental conditions, implying that other actions of H_2O_2 are also required.

Fig. 2C shows that EAD amplitude after H_2O_2 depended on its take-off potential during repolarization, such that the more repolarized the take-off potential, the larger the EAD

amplitude. This relationship parallels the voltage dependence of $I_{Ca,L}$ reactivation and the $I_{Ca,L}$ window current [24, 25]. Consistent with this interpretation, the selective $I_{Ca,L}$ blocker nifedipine (10 μM) eliminated EADs (Fig. 2D), even though APD remained markedly prolonged due to the effect of H_2O_2 on late I_{Na} (as indicated by shortening of APD with subsequent application of 10 μM TTX or 20 μM ranolazine). Taken together, these results suggest that at least two actions of H_2O_2 are required for EAD formation: activation of late I_{Na} to reduce repolarization reserve (i.e. prolong APD) and modification of $I_{Ca,L}$ to enhance its reactivation properties so as to generate the EAD upstroke.

Whereas the effects of H_2O_2 on late I_{Na} have been well documented in previous studies [4, 5], the reported effects of H_2O_2 on $I_{Ca,L}$ have been variable. Therefore, we examine how H_2O_2 affected $I_{Ca,L}$ in rabbit ventricular myocytes under our experimental conditions. Fig. 3A and B show the time course of both peak $I_{Ca,L}$ and the residual pedestal $I_{Ca,L}$ at the end of a 300ms voltage clamp to 0 mV in a representative myocyte during exposure to 1 mM H_2O_2. Both peak and pedestal $I_{Ca,L}$ increased, from 7.3 ± 0.8 to 12.1 ± 1.8 pA/pF (n=5) and from 0.5 ± 0.1 to 3.2 ± 0.3 pA/pF (n=5), respectively. To examine how these changes affect $I_{Ca,L}$ during the repolarization phase of the AP, we performed AP clamp experiments before and after exposure to 1 mM H_2O_2. Fig. 3C shows that H_2O_2 induced a prominent $I_{Ca,L}$ hump during the late phase of the AP plateau, consistent with the timing of the EAD (compare to Fig. 1 &2). The recordings shown in Fig. 3 B & C represent the nifedipine-sensitive (subtracted) current, indicating that the increase of the inward current (including the hump in the late phase) is mostly due to $I_{Ca,L}$, although minor contamination by the Na-Ca exchange current (I_{NCX}) cannot be excluded.

The role of Ca_i cycling

After H_2O_2 exposure, we often observed a transient inward current (I_{ti}) following repolarization to -80 mV (Fig. 4A and inset), consistent with spontaneous SR Ca release as a result of the enhanced Ca influx via $I_{Ca,L}$ causing SR Ca overload. To investigate the relationship to the EAD-induced DADs observed in Fig. 1, we simultaneously imaged Ca_i in Fluo-4-AM loaded myocytes (Fig. 4B-D). During H_2O_2-induced EADs, Ca_i remained elevated (Fig. 4C) or increased (Fig. 4D), consistent with additional SR Ca release due to reactivation of $I_{Ca,L}$. The line scan in Fig. 4D shows that the rise in Ca_i during the second EAD was not spatially homogeneous. This may indicate that Ca-induced Ca release from the SR, in addition to $I_{Ca,L}$ enhancement, contributed to EAD formation by enhancing I_{ti} (since H_2O_2 has been reported to enhance Na-Ca exchange [14]). Fig. 4D documents that after repolarization, a spontaneous Ca_i wave originating from the center of the cell and propagating towards both ends was associated with a DAD. This can be attributed to increased SR Ca loading during the preceding AP, which was markedly prolonged by EADs.

To further investigate the role of Ca_i cycling in H_2O_2-induced afterdepolarizations, we examined the effects of pre-loading myocytes with BAPTA-AM to buffer changes in Ca_i (Fig. 5A). We also pre-treated myocytes with thapsigargin (0.2 μM) and ryanodine (10 μM) to suppress SR Ca cycling (Fig. 5B). Both interventions completely prevented EADs and DADs during exposure to 1 mM H_2O_2 (Fig. 5), indicating the intact Ca_i cycling plays a critical role. However, APD remained prolonged under these conditions, probably due to reduced Ca-induced inactivation of $I_{Ca,L}$ when the intracellular Ca_i transient was suppressed [26].

The role of CaMKII signaling

Similar to the effects of H_2O_2, Ca^{2+}-dependent CaMKII activation has been shown to modify I_{Na} inactivation, enhance $I_{Ca,L}$, and promote EADs [19-21]. CaMKII could either be activated by Ca_i, due to the effects of H_2O_2 on Ca_i cycling proteins, or directly by oxidative stress, as shown recently in cardiac myocytes [16, 18]. The Ca_i-dependence is still consistent H_2O_2-mediated activation of CaMKII, since persistent activation of CaMKII by oxidation requires Ca-CaM

binding to CaMKII to expose its redox sites [18]. We examined the effects of CaMKII inhibition to test these possibilities. Pretreatment with the CaMK inhibitor KN-93 (1 μM) prevented the emergence of EADs during exposure to H_2O_2 (1 mM for up to 20-30 min) in 4 myocytes (Fig. 6A), compared to non-pretreated myocytes in which H_2O_2 (1 mM) consistently induced EADs within 5-10 min of H_2O_2 exposure (Fig. 1A, 6B). In addition, KN-93 also suppressed EADs after they were induced by H_2O_2 perfusion (Fig. 6B).

In contrast, 1μM KN-92, an inactive analog of KN-93, was ineffective (Fig. 7A and B), with EADs appearing after an average of 7.5 ± 1.2 min (n = 5) after exposure to 1 mM H_2O_2 (n=5). BAPTA-AM, however, remained effective at suppressing H_2O_2-induced EADs in the presence of KN-92 (Fig. 7B).

Since both KN-93 and KN-92 have nonspecific effects, such as blockade of Ca and K currents [22, 27, 28], we also examined the effects of the selective CaMKII inhibitor peptide AIP (2 μM). In 8 myocytes, AIP added to patch pipette dialyzing the cytoplasm delayed the appearance of EADs during exposure to 200 μM H_2O_2, from 6.6 ± 0.8 (n=10) to 13.9 ± 2.7 mins (Fig 6C) ($p<0.05$). Moreover, AIP dialysis also prolonged APD in a concentration-dependent manner, presumably due to nonspecific peptide effects, such that higher AIP concentrations were ineffective at preventing H_2O_2-induced EADs.

Discussion

In the present study, we investigated the mechanisms by which oxidative stress caused by exposure to H_2O_2 induces afterdepolarization and triggered activity in rabbit ventricular myocytes. The novel findings are: 1) $I_{Ca,L}$ modification, in addition to I_{Na} modification, plays a crucial role in EAD generation by H_2O_2; 2) CaMKII activation, either directly via oxidative stress, or indirectly via elevated Ca_i, is critical for these effects; 3) By enhancing SR Ca loading and promoting spontaneous Ca_i waves, H_2O_2–induced EADs also cause DADs, providing a direct link between these two types of afterdepolarizations which compounds the arrhythmogenic potential of oxidative stress.

Ionic mechanisms of EADs and DADs induced by H_2O_2

Two conditions are required to generate an EAD. First, repolarization reserve must be reduced during phases 2 & 3 of the AP, by an increase in inward current, a decrease in outward current, or both. Second, once repolarization reserve has been compromised, reactivation of $I_{Ca,L}$ window current, and/or additional SR Ca release augmenting Ca-sensitive inward currents such as I_{NCX}, must be sufficiently powerful to reverse repolarization and generate the EAD upstroke. In ventricular muscle, inward currents influencing repolarization reserve include I_{Na}, I_{CaL}, and I_{NCX}, while outward currents include the rapid and slow delayed rectifier K^+ currents (I_{Kr}, and I_{Ks}), the transient outward current (I_{to}) and the inward rectifier potassium current (I_{K1}). Previous studies analyzing the mechanisms of H_2O_2-induced EADs have implicated impaired I_{Na} inactivation as the primary mechanism reducing repolarization reserve [4, 5]. However, H_2O_2 has also been reported to affect other currents and transporters. In the present study, we show that in addition to modification of I_{Na}, modification of $I_{Ca,L}$ by H_2O_2 plays a key role in EAD genesis. Not only did H_2O_2 substantially increase the peak amplitude of $I_{Ca,L}$, but it also impaired $I_{Ca,L}$ inactivation (increase of pedestal current as shown in Fig. 3A & B). The consequence was a large increase in the late phase of $I_{Ca,L}$, as seen during the AP clamp in Fig. 3C, which was not successfully overcome by outward currents, accounting for the genesis of the EAD. The experiments using multiple ion channel blockers (Fig, 2) showed that despite prolonging APD, I_{Na} modification was not by itself sufficient to induce EADs when $I_{Ca,L}$ was blocked. Both I_{Na} and $I_{Ca,L}$ modification could be attributed to CaMKII activation, since, as shown in Fig. 6A, H_2O_2 failed to prolong APD significantly or cause EADs when CaMKII was blocked by KN-93.

Oxidative stress also modulates the properties of other Ca_i-cycling proteins, including ryanodine receptors [11, 12] and SERCA2a [13], which could potentially promote EAD genesis by modulating SR Ca release during repolarization. Indeed, some recent studies have shown that EADs and DADs can share a common mechanism under Ca_i overload conditions [29-31]. Non-$I_{Ca,L}$-gated SR Ca^{2+}-release during repolarization has been proposed to contribute to EAD genesis by activating Ca-sensitive inward currents [29], but it is difficult to unequivocally distinguish from SR Ca release triggered by reactivated L-type Ca channels.

It has been reported that voltage can directly activate SR Ca^{2+}-release in cardiac myocytes, which is enhanced by cAMP [32, 33]. However, EADs were readily induced by H_2O_2 using cAMP-free pipette solution (data not shown, also see Song et al[5]), excluding an essential role of a cAMP-sensitive voltage-activated Ca release in EAD generation.

Contribution of SR Ca handling to the EADs and DADs induced by H_2O_2

CaMKII can phosphorylate RyR2, which may enhance SR Ca release dependent triggered activity [34]. However, while it is well accepted that CaMKII phosphorylates RyR2, the functional consequences are controversial. Bers' group found increased SR Ca leak from CaMKII-mediated RyR2 phosphorylation [34, 35], but Yang et al [36] reported a suppression of Ca sparks and Ca waves. The cause of this discrepancy remains to be determined. In addition, oxidative stress has direct effects on RyR and SR function. The interdependencies between SR Ca cycling, $I_{Ca,L}$, I_{NCX}, and repolarization reserve are complex and nonlinear, making it very challenging, if not impossible, to assign a simple mechanistic role of SR Ca cycling to EAD generation. For example, SR depletion could suppress EADs by any of the following interactive mechanisms: 1) preventing CaMKII activation by oxidative stress (since the Ca-CaM interaction is still required); 2) increasing repolarization reserve by suppressing I_{NCX}; 3) preventing Ca waves during the repolarization phase; 4) altering activation/inactivation properties of other ionic currents.

In the presence of BAPTA, the AP has a higher rectangular plateau (Fig. 5), which may also hinder the reactivation of $I_{Ca,L}$ and EAD formation, consistent with a recent study showing that triangulation of the AP favors $I_{Ca,L}$ reactivation [37].

The Role of CaMKII Signaling in H_2O_2-induced EADs

The enhancement of $I_{Ca,L}$ by H_2O_2 in the present study is consistent with activation of CaMKII by H_2O_2, although direct redox modifications of L-type Ca channel subunits may also contribute. CaMKII is known to mediate $I_{Ca,L}$ facilitation [38], and CaMKII activation has been shown to promote EADs in a variety of settings [19, 22]. Moreover, CaMKII activation has recently been reported to impair I_{Na} inactivation [21], consistent with a common underlying pathogenesis of H_2O_2-induced and CaMKII-induced EADs. Our finding that the CaMKII inhibitor KN-93, but not its inactive analog KN-92, suppressed EAD formation by H_2O_2, generally supports a common mechanism. On the other hand, both KN-93 and KN-92 have nonspecific effects, including substantial block of $I_{Ca,L}$[27] which is critical in EAD formation. However, the selective CaMKII peptide inhibitor AIP also significantly delayed the onset of EADs during exposure to 0.2 mM H_2O_2. Theoretically, AIP should be equally effective at preventing CaMKII activation by oxidative stress as by elevated Ca_i, since both activation modes require initial interaction of CaMKII's regulatory domain with Ca-CaM complexes, to expose the redox and autophosphorylation sites on CaMKII's catalytic domain [18]. This also explains why BAPTA-AM prevents EADs during H_2O_2 exposure, by preventing Ca_i from rising sufficiently for Ca-CaM to interact with CaMKII and trigger the subsequent persistent activation by redox modification.

Based on these observations, the role of CaMKII activation in H_2O_2-induced EADs can be summarized as follows: 1) CaMKII activation by H_2O_2 contributes to both impaired I_{Na} inactivation and $I_{Ca,L}$ facilitation; 2) Both factors enhance cellular Ca loading by prolonging APD and increasing Ca influx via $I_{Ca,L}$, promoting further CaMKII activation via Ca-CaM; 3) KN-93 synergistically suppresses EADs by preventing CaMKII activation by H_2O_2 and reducing Ca influx by directly blocking $I_{Ca,L}$. Without concomitantly inhibiting CaMKII activation, partial block of $I_{Ca,L}$ by KN-92 is not sufficient to suppress EAD formation; 4) Direct redox modification of ion channel proteins may also contribute, since selective CaMKII inhibition with AIP delayed the onset of, but did not entirely suppress, H_2O_2-induced EADs. We do not have a ready explanation for why AIP showed less effectiveness than KN-93 in our present study. KN-93 also blocks the L-type Ca current upon which EAD generation depends, which may account for its more complete potency. Alternatively, AIP may have had nonspecific effects which reduced repolarization reserve, since it modestly prolonged APD.

EAD-associated DADs

Associations between EADs and DADs have been noted previously [6, 31, 39, 40], but the underlying mechanisms have not been analyzed in detail. For example, in atrial myocytes, Song et al [40] found that ATX-induced EADs were also associated with DADs. They postulated that DADs were due to excessive Ca-loading as a result of APD prolongation by EADs, leading to spontaneous SR Ca release following repolarization. Here we directly documented this postulated mechanism for H_2O_2-induced EADs, by using optical Ca_i imaging to detect the spontaneous Ca_i wave inducing a transient inward current causing the DAD (Fig. 4). It is also conceivable that oxidative stress directly sensitizes the SR to non $I_{Ca,L}$-gated SR Ca^{2+}-release through direct effects on Ca_i cycling proteins such as RyR [11, 12], but this remains to be established. In either case, our findings suggest that both EADs and EAD-induced DADs may both contribute to TA during oxidative stress, amplifying the arrhythmogenic consequences.

Clinical Implications

Increased oxidative stress is believed to be an important factor predisposing the diseased heart to lethal arrhythmias. Here we have shown how oxidative stress caused by exogenous H_2O_2 predisposes the heart to both EADs and DADs, and demonstrated a link to CaMKII activation, which is also involved in other aspects of heart failure [41, 42]. Other free radical sources have also been reported to produce similar results, i.e. inducing EADs, DADs and triggered activities [6]. Although it is still under debate, H_2O_2 levels up to ~35 μM have been reported in human blood plasma [43]. It is also well known that ROS levels can increase during ischemia and reperfusion by as much as 100-fold [44], and also with age by 7.5 fold [45]. Since ROS are short-lived radicals, it is conceivable that the local concentrations near sites of production are considerably higher than circulating concentrations. Therefore, the concentrations (100-200 μM) used in most of our experiments are reasonable approximations of the pathophysiologically relevant range. Targeting CaMKII signaling may have therapeutic potential to prevent arrhythmias in the failing heart, although negative inotropic actions [46] may limit the use of CaMKII inhibitors.

Acknowledgments

Sources of Funding: The study was supported by NIH/NHLBI grants P50 HL53219 and P01 HL078931, and Laubisch and Kawata Endowments.

References

1. Lakatta EG, Sollott SJ. The “heartbreak” of older age. Mol Interv 2002;2:431–446. [PubMed: 14993406]

2. Slezak J, Tribulova N, Pristacova J, Uhrik B, Thomas T, Khaper N, Kaul N, Singal PK. Hydrogen peroxide changes in ischemic and reperfused heart. Cytochemistry and biochemical and X-ray microanalysis. Am J Pathol 1995;147:772–781. [PubMed: 7677188]
3. Corretti MC, Koretsune Y, Kusuoka H, Chacko VP, Zweier JL, Marban E. Glycolytic inhibition and calcium overload as consequences of exogenously generated free radicals in rabbit hearts. J Clin Invest 1991;88:1014–1025. [PubMed: 1653271]
4. Ward CA, Giles WR. Ionic mechanism of the effects of hydrogen peroxide in rat ventricular myocytes. J Physiol 1997;500:631–642. [PubMed: 9161981]
5. Song Y, Shryock JC, Wagner S, Maier LS, Belardinelli L. Blocking late sodium current reduces hydrogen peroxide-induced arrhythmogenic activity and contractile dysfunction. J Pharmacol Exp Ther 2006;318:214–222. [PubMed: 16565163]
6. Barrington PL, Meier CF Jr, Weglicki WB. Abnormal electrical activity induced by H2O2 in isolated canine myocytes. Basic Life Sci 1988;49:927–932. [PubMed: 3250541]
7. Guo J, Giles WR, Ward CA. Effect of hydrogen peroxide on the membrane currents of sinoatrial node cells from rabbit heart. Am J Physiol Heart Circ Physiol 2000;279:H992–999. [PubMed: 10993760]
8. Hudasek K, Brown ST, Fearon IM. H2O2 regulates recombinant Ca2+ channel alpha1C subunits but does not mediate their sensitivity to acute hypoxia. Biochem Biophys Res Commun 2004;318:135–141. [PubMed: 15110764]
9. Goldhaber JI, Liu E. Excitation-contraction coupling in single guinea-pig ventricular myocytes exposed to hydrogen peroxide. J Physiol 1994;477:135–147. [PubMed: 8071880]
10. Berube J, Caouette D, Daleau P. Hydrogen peroxide modifies the kinetics of HERG channel expressed in a mammalian cell line. J Pharmacol Exp Ther 2001;297:96–102. [PubMed: 11259532]
11. Anzai K, Ogawa K, Ozawa T, Yamamoto H. Oxidative modification of ion channel activity of ryanodine receptor. Antioxid Redox Signal 2000;2:35–40. [PubMed: 11232597]
12. Zissimopoulos S, Docrat N, Lai FA. Redox sensitivity of the ryanodine receptor interaction with FK506-binding protein. J Biol Chem 2007;282:6976–6983. [PubMed: 17200109]
13. Morris TE, Sulakhe PV. Sarcoplasmic reticulum Ca(2+)-pump dysfunction in rat cardiomyocytes briefly exposed to hydroxyl radicals. Free Radic Biol Med 1997;22:37–47. [PubMed: 8958128]
14. Hinata M, Matsuoka I, Iwamoto T, Watanabe Y, Kimura J. Mechanism of Na+/Ca2+ exchanger activation by hydrogen peroxide in guinea-pig ventricular myocytes. J Pharmacol Sci 2007;103:283–292. [PubMed: 17332693]
15. Goldhaber JI. Free radicals enhance Na+/Ca2+ exchange in ventricular myocytes. Am J Physiol 1996;271:H823–833. [PubMed: 8853314]
16. Zhu W, Woo AY, Yang D, Cheng H, Crow MT, Xiao RP. Activation of CaMKIIdeltaC is a common intermediate of diverse death stimuli-induced heart muscle cell apoptosis. J Biol Chem 2007;282:10833–10839. [PubMed: 17296607]
17. Howe CJ, Lahair MM, McCubrey JA, Franklin RA. Redox regulation of the calcium/calmodulin-dependent protein kinases. J Biol Chem 2004;279:44573–44581. [PubMed: 15294913]
18. Erickson JR, Joiner ML, Guan X, Kutschke W, Yang J, Oddis CV, Bartlett RK, Lowe JS, O'Donnell SE, Aykin-Burns N, Zimmerman MC, Zimmerman K, Ham AJ, Weiss RM, Spitz DR, Shea MA, Colbran RJ, Mohler PJ, Anderson ME. A dynamic pathway for calcium-independent activation of CaMKII by methionine oxidation. Cell 2008;133:462–474. [PubMed: 18455987]
19. Wu Y, Temple J, Zhang R, Dzhura I, Zhang W, Trimble R, Roden DM, Passier R, Olson EN, Colbran RJ, Anderson ME. Calmodulin kinase II and arrhythmias in a mouse model of cardiac hypertrophy. Circulation 2002;106:1288–1293. [PubMed: 12208807]
20. Wu Y, MacMillan LB, McNeill RB, Colbran RJ, Anderson ME. CaM kinase augments cardiac L-type Ca2+ current: a cellular mechanism for long Q-T arrhythmias. Am J Physiol 1999;276:H2168–2178. [PubMed: 10362701]
21. Wagner S, Dybkova N, Rasenack EC, Jacobshagen C, Fabritz L, Kirchhof P, Maier SK, Zhang T, Hasenfuss G, Brown JH, Bers DM, Maier LS. Ca2+/calmodulin-dependent protein kinase II regulates cardiac Na+ channels. J Clin Invest 2006;116:3127–3138. [PubMed: 17124532]
22. Anderson ME, Braun AP, Wu Y, Lu T, Schulman H, Sung RJ. KN-93, an inhibitor of multifunctional Ca++/calmodulin-dependent protein kinase, decreases early afterdepolarizations in rabbit heart. J Pharmacol Exp Ther 1998;287:996–1006. [PubMed: 9864285]

23. Mantegazza M, Franceschetti S, Avanzini G. Anemone toxin (ATX II)-induced increase in persistent sodium current: effects on the firing properties of rat neocortical pyramidal neurones. J Physiol 1998;507:105–116. [PubMed: 9490824]
24. January CT, Riddle JM, Salata JJ. A model for early afterdepolarizations: induction with the Ca2+ channel agonist Bay K 8644. Circ Res 1988;62:563–571. [PubMed: 2449297]
25. January CT, Riddle JM. Early afterdepolarizations: mechanism of induction and block. A role for L-type Ca2+ current. Circ Res 1989;64:977–990. [PubMed: 2468430]
26. Pott C, Yip M, Goldhaber JI, Philipson KD. Regulation of cardiac L-type Ca2+ current in Na+-Ca2+ exchanger knockout mice: functional coupling of the Ca2+ channel and the Na+-Ca2+ exchanger. Biophys J 2007;92:1431–1437. [PubMed: 17114214]
27. Gao L, Blair LA, Marshall J. CaMKII-independent effects of KN93 and its inactive analog KN92: reversible inhibition of L-type calcium channels. Biochem Biophys Res Commun 2006;345:1606–1610. [PubMed: 16730662]
28. Rezazadeh S, Claydon TW, Fedida D. KN-93 (2-[N-(2-hydroxyethyl)]-N-(4-methoxybenzenesulfonyl)]amino-N-(4-chlorocinn amyl)-N-methylbenzylamine), a calcium/calmodulin-dependent protein kinase II inhibitor, is a direct extracellular blocker of voltage-gated potassium channels. J Pharmacol Exp Ther 2006;317:292–299. [PubMed: 16368898]
29. Choi BR, Burton F, Salama G. Cytosolic Ca2+ triggers early afterdepolarizations and Torsade de Pointes in rabbit hearts with type 2 long QT syndrome. J Physiol 2002;543:615–631. [PubMed: 12205194]
30. Salama G. Arrhythmia genesis: aberrations of voltage or Ca2+ cycling? Heart Rhythm 2006;3:67–70. [PubMed: 16399056]
31. Volders PG, Kulcsar A, Vos MA, Sipido KR, Wellens HJ, Lazzara R, Szabo B. Similarities between early and delayed afterdepolarizations induced by isoproterenol in canine ventricular myocytes. Cardiovasc Res 1997;34:348–359. [PubMed: 9205549]
32. Ferrier GR, Howlett SE. Cardiac excitation-contraction coupling: role of membrane potential in regulation of contraction. Am J Physiol Heart Circ Physiol 2001;280:H1928–1944. [PubMed: 11299192]
33. Hobai IA, Howarth FC, Pabbathi VK, Dalton GR, Hancox JC, Zhu JQ, Howlett SE, Ferrier GR, Levi AJ. “Voltage-activated Ca release” in rabbit, rat and guinea-pig cardiac myocytes, and modulation by internal cAMP. Pflugers Arch 1997;435:164–173. [PubMed: 9359916]
34. Guo T, Zhang T, Mestril R, Bers DM. Ca2+/Calmodulin-dependent protein kinase II phosphorylation of ryanodine receptor does affect calcium sparks in mouse ventricular myocytes. Circ Res 2006;99:398–406. [PubMed: 16840718]
35. Curran J, Hinton MJ, Rios E, Bers DM, Shannon TR. Beta-adrenergic enhancement of sarcoplasmic reticulum calcium leak in cardiac myocytes is mediated by calcium/calmodulin-dependent protein kinase. Circ Res 2007;100:391–398. [PubMed: 17234966]
36. Yang D, Zhu WZ, Xiao B, Brochet DX, Chen SR, Lakatta EG, Xiao RP, Cheng H. Ca2+/calmodulin kinase II-dependent phosphorylation of ryanodine receptors suppresses Ca2+ sparks and Ca2+ waves in cardiac myocytes. Circ Res 2007;100:399–407. [PubMed: 17234969]
37. Guo D, Zhao X, Wu Y, Liu T, Kowey PR, Yan GX. L-type calcium current reactivation contributes to arrhythmogenesis associated with action potential triangulation. J Cardiovasc Electrophysiol 2007;18:196–203. [PubMed: 17212595]
38. Wu Y, Kimbrough JT, Colbran RJ, Anderson ME. Calmodulin kinase is functionally targeted to the action potential plateau for regulation of L-type Ca2+ current in rabbit cardiomyocytes. J Physiol 2004;554:145–155. [PubMed: 14678498]
39. Priori SG, Corr PB. Mechanisms underlying early and delayed afterdepolarizations induced by catecholamines. Am J Physiol 1990;258:H1796–1805. [PubMed: 2163219]
40. Song Y, Shryock JC, Belardinelli L. An increase of late sodium current induces delayed afterdepolarizations and sustained triggered activity in atrial myocytes. Am J Physiol Heart Circ Physiol 2008;294:H2031–2039. [PubMed: 18310511]
41. Bers DM, Guo T. Calcium signaling in cardiac ventricular myocytes. Ann N Y Acad Sci 2005;1047:86–98. [PubMed: 16093487]

42. Couchonnal LF, Anderson ME. The role of calmodulin kinase II in myocardial physiology and disease. Physiology (Bethesda) 2008;23:151–159. [PubMed: 18556468]

43. Halliwell B, Clement MV, Long LH. Hydrogen peroxide in the human body. FEBS Lett 2000;486:10–13. [PubMed: 11108833]

44. Dhalla NS, Duhamel TA. The paradoxes of reperfusion in the ischemic heart. Heart Metab 2007;37:31–34.

45. Maurel A, Hernandez C, Kunduzova O, Bompart G, Cambon C, Parini A, Frances B. Age-dependent increase in hydrogen peroxide production by cardiac monoamine oxidase A in rats. Am J Physiol Heart Circ Physiol 2003;284:H1460–1467. [PubMed: 12531732]

46. Maier LS, Bers DM. Role of Ca2+/calmodulin-dependent protein kinase (CaMK) in excitation-contraction coupling in the heart. Cardiovasc Res 2007;73:631–640. [PubMed: 17157285]

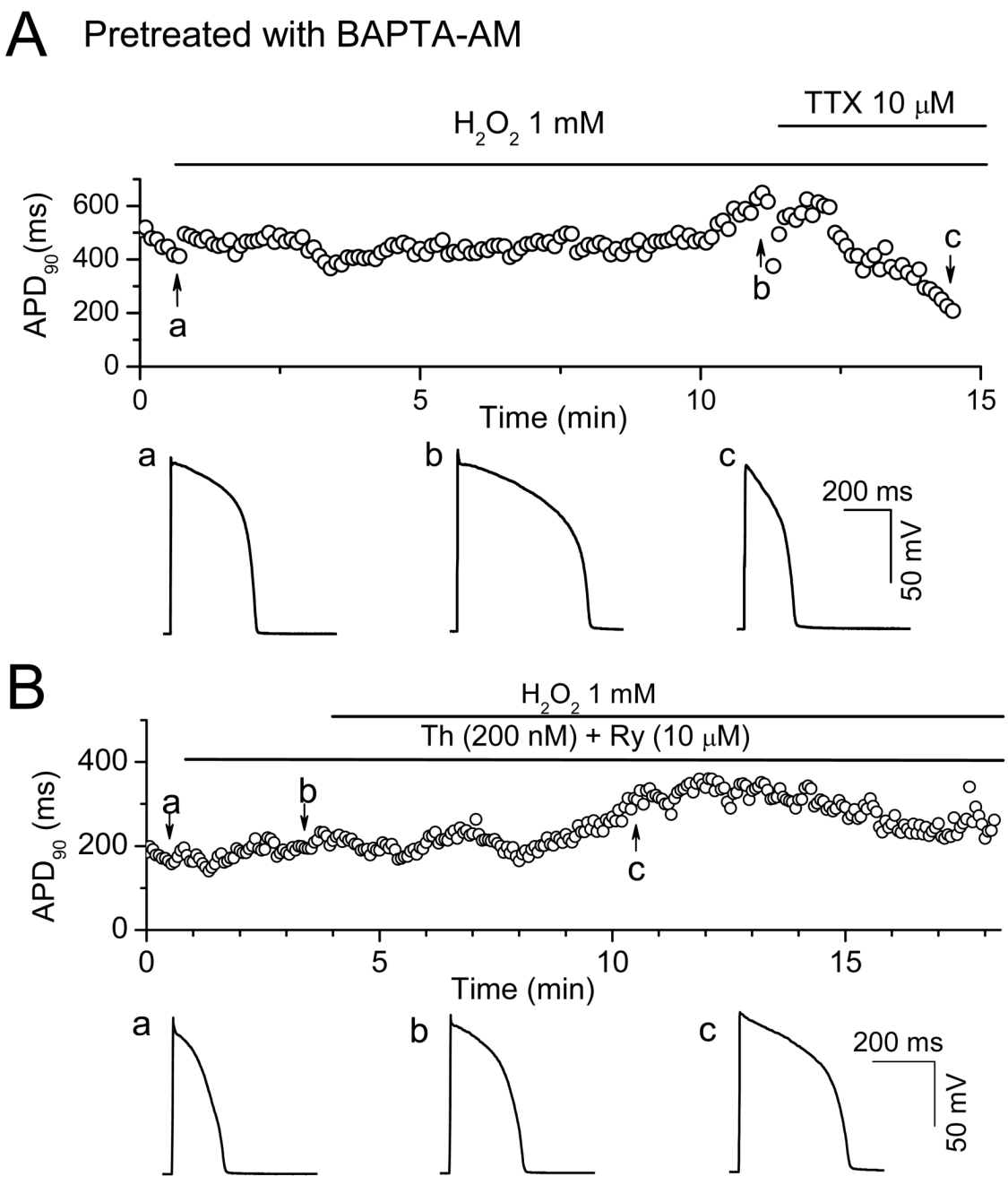

Fig. 1. Afterdepolarizations and triggered activity during H_2O_2 exposure in isolated rabbit ventricular myocytes

A. Action potentials (APs) were elicited with 2 ms-2nA pulses under current clamp conditions at pacing cycle length (PCL) of 6 sec. Values of consecutive APD_{90} are plotted over time. H_2O_2 (200 μM) was perfused continuously as indicated by the horizontal bar above the plot. EADs are indicated by the sudden and dramatic increases of APD_{90} (at ~ 6 min after H_2O_2 application). Insets show APs under control condition, and after H_2O_2 with an EAD. **B.** Examples of afterdepolarizations and TA during exposure to 1 mM H_2O_2, including multiple oscillatory EADs (left panel), an EAD followed by a DAD (middle panel), and an EAD followed by a DAD causing TA (right panel). **C.** Successive APs recorded during H_2O_2

exposure, illustrating the irregular occurrence of EADs (asterisks) and associated DADs (arrows).

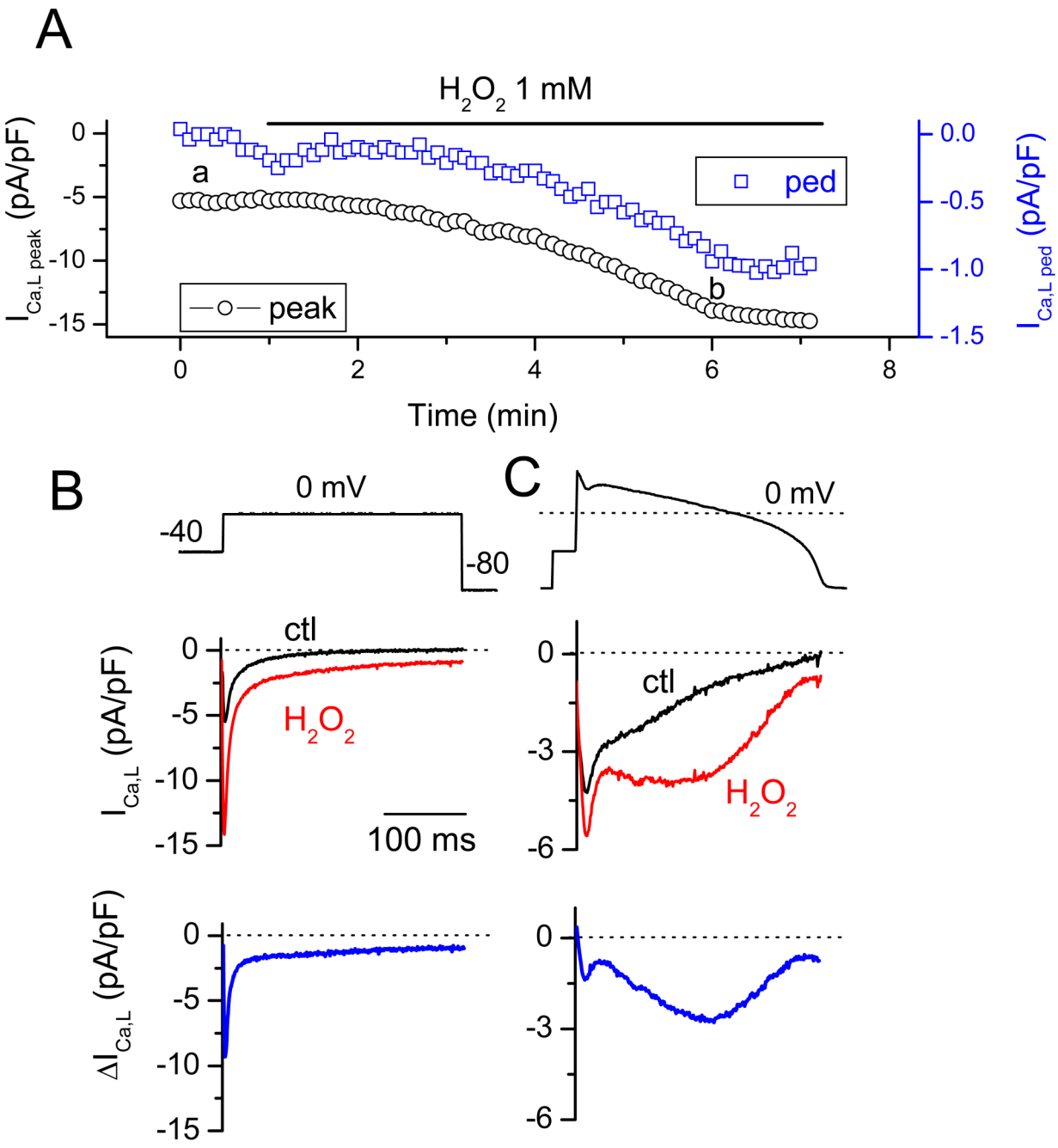

Fig. 2. The involvement of both I_{Na} and $I_{Ca,L}$ in H_2O_2-induced EAD

A. The specific I_{Na} blocker TTX (10 μM) reversibly suppressed EADs and shortened APD. **B.** ATX (30 nM), a selective activator of persistent I_{Na}, prolonged APD but did not generate cause frank EADs with a distinct upstroke. **C.** The amplitude of H_2O_2-induced EADs depended on their take-off potentials (arrows). **D.** The $I_{Ca,L}$ blocker nifedipine (Nif, 10 μM) suppressed the EAD upstroke, although AP plateau remained prolonged, unless TTX (10 μM) was also added.

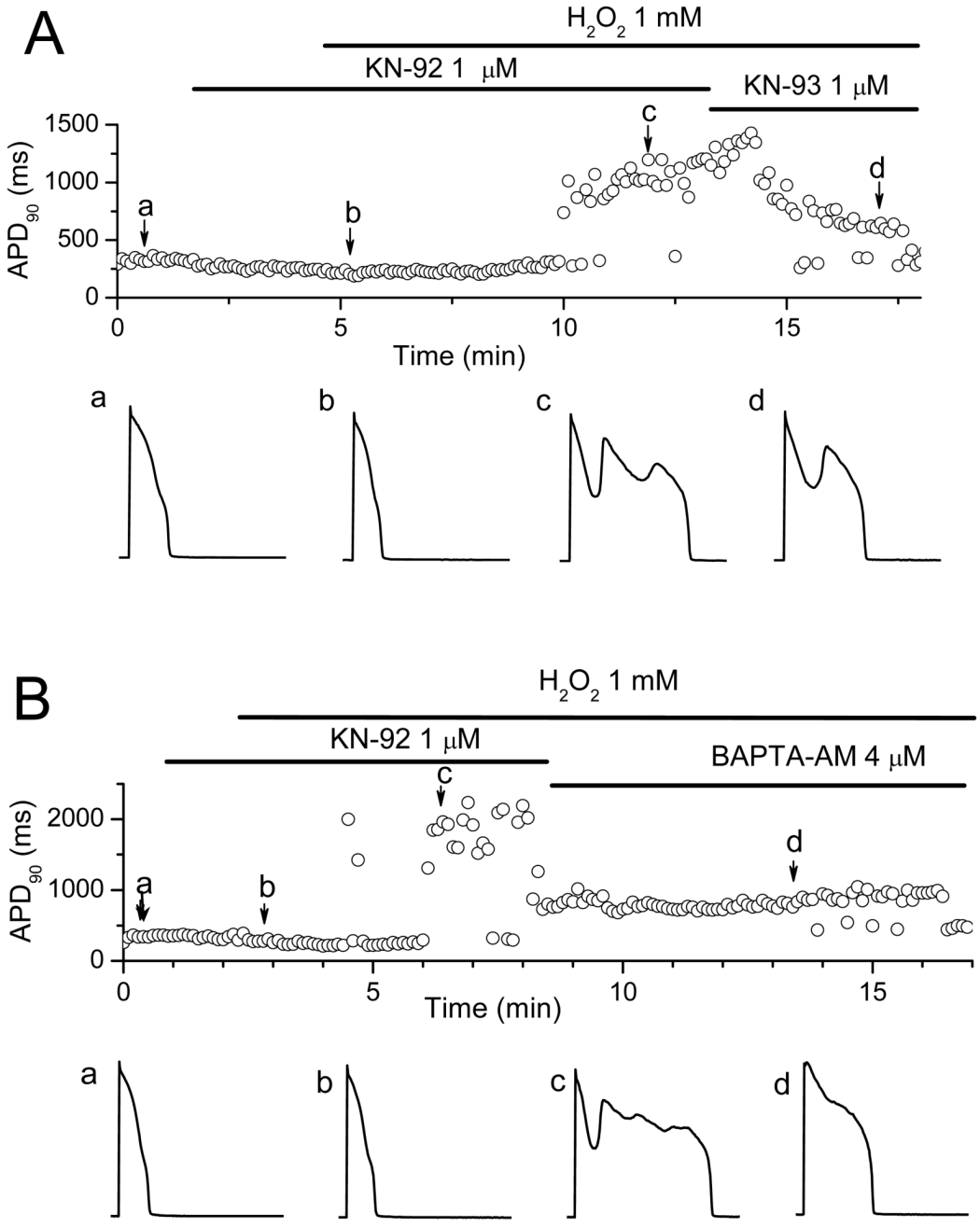

Fig. 3. Enhancement of $I_{Ca,L}$ by H_2O_2

A. Time course of the peak and residual pedestal (ped) $I_{Ca,L}$ during a 300 ms voltage clamp pulse to 0 mV (voltage protocol shown in B). **B.** Voltage clamp pulse (above) and superimposed current traces showing $I_{Ca,L}$ before (black) and ~5 min after perfusion of 1mM H_2O_2 (red). The difference current is shown in the bottom trace. **C.** Same as B, but with an AP clamp waveform replacing the square voltage clamp pulse.

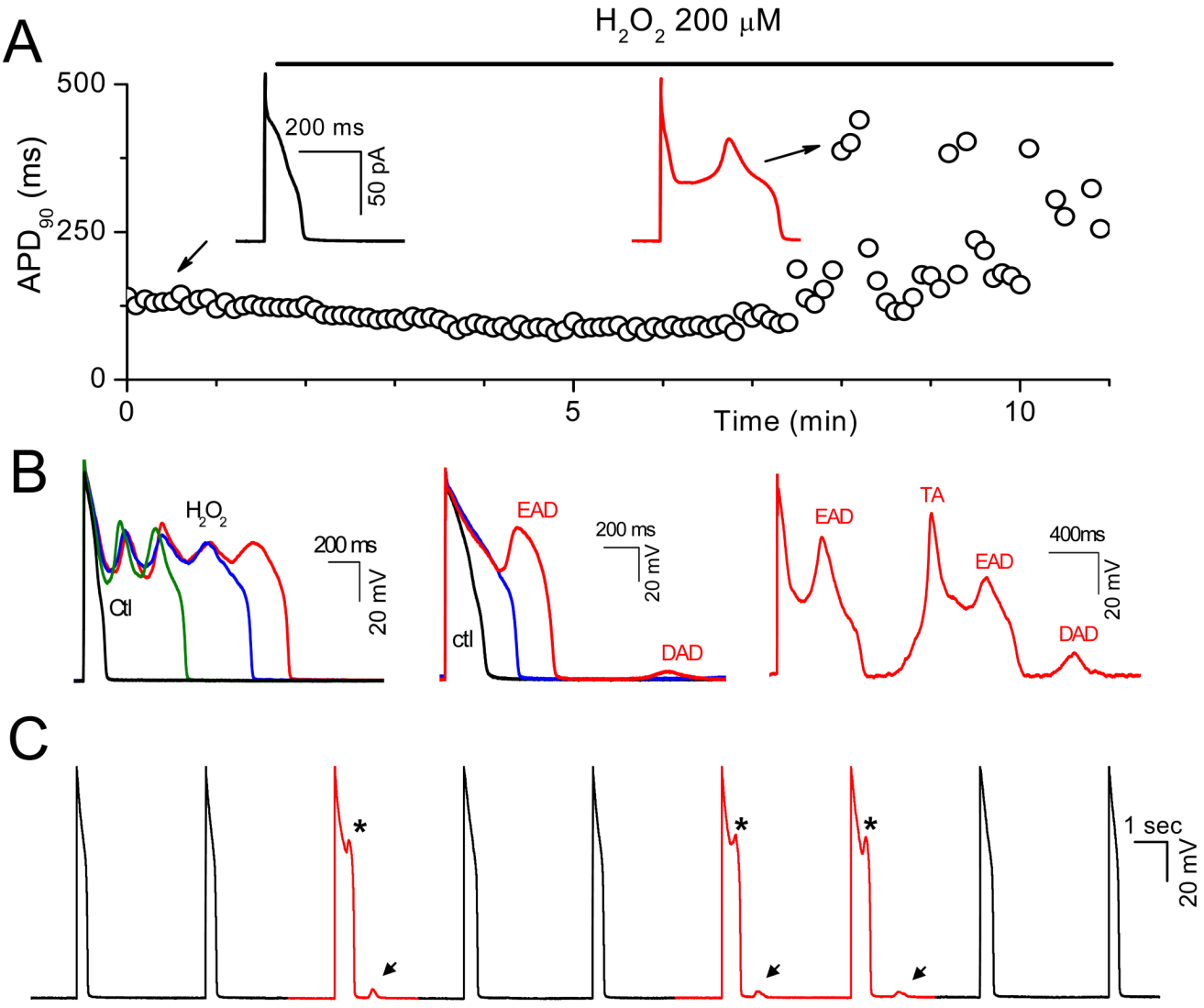

Fig. 4. Transient inward current (I_{ti}) and Ca_i transients during H_2O_2–induced EADs and DADs

A. Similar to Fig. 3B, but with an I_{ti} following repolarization to -80 mV in the presence of H_2O_2 (expanded in bottom trace). **B.** AP (top), simultaneous whole-cell Ca_i transient (middle), and a line-scan image along the long axis of the myocyte (bottom) before H_2O_2. **C & D**. Same following H_2O_2 exposure. In C, two EADs occur, leading to persistent elevation in Ca_i and additional Ca^{2+} release (r) during the second EAD. In D (different cell), two EADs (associated with additional $I_{Ca,L}$-gated SR Ca^{2+}-release) are followed by a DAD due to a non-voltage gated spontaneous Ca_i wave (w) starting from the middle of the cell (*).

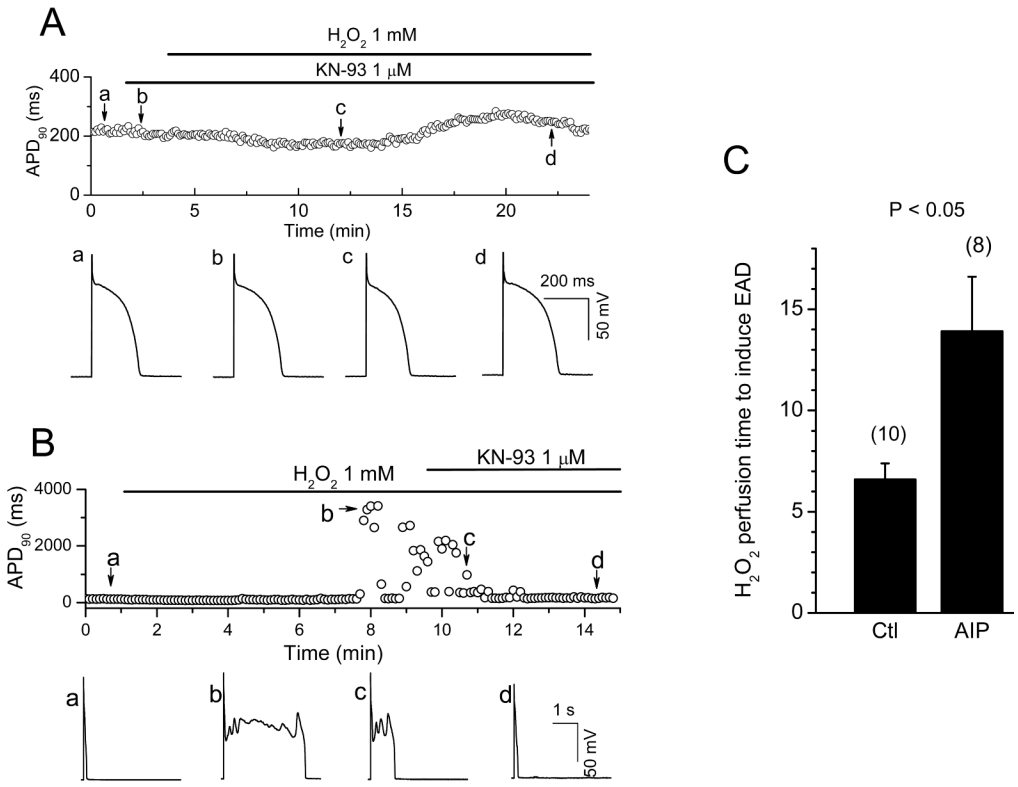

Fig. 5. Dependence of H_2O_2-induced EADs on intact Ca_i cycling

A. Time course of APD_{90} in a myocyte preloaded with BAPTA-AM (4 μM) for 30 min exposure to 1 mM H_2O_2. Representative APs at points a (control), b (~10 min in H_2O_2), and c (H_2O_2 + TTX) are shown below. **B.** Same, but in a myocyte pre-treated with 10 μM Ryanodine (Ry) + 200 nM Thapsigargin (Th) prior to H_2O_2.

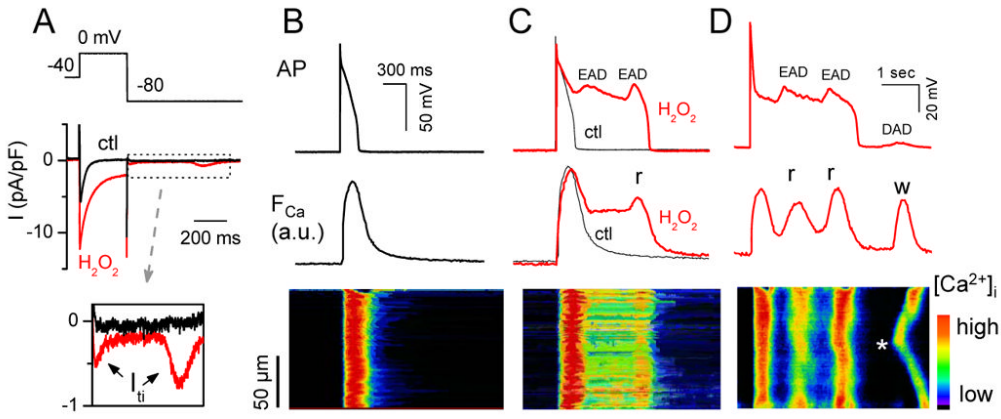

Fig. 6. Suppression of H_2O_2–induced EADs by the CaMKII inhibitor KN-93 and AIP

A. Time course of APD_{90} in a myocyte treated with the CaMKII inhibitor KN-93 prior to exposure to 1 mM H_2O_2. APs under control (a), in the presence of KN-93 and after perfusion with KN93 + H_2O_2 for 9 min (c) and 19 min (d) are shown in the lower panels. **B**. Same, but with KN-93 applied after EADs were induced by H_2O_2. In both protocols, KN-93 suppressed EADs. **C**. Bar graph showing the average H_2O_2 (200 µM) perfusion time to cause EAD appearance in the absence and presence of 2 µM AIP.

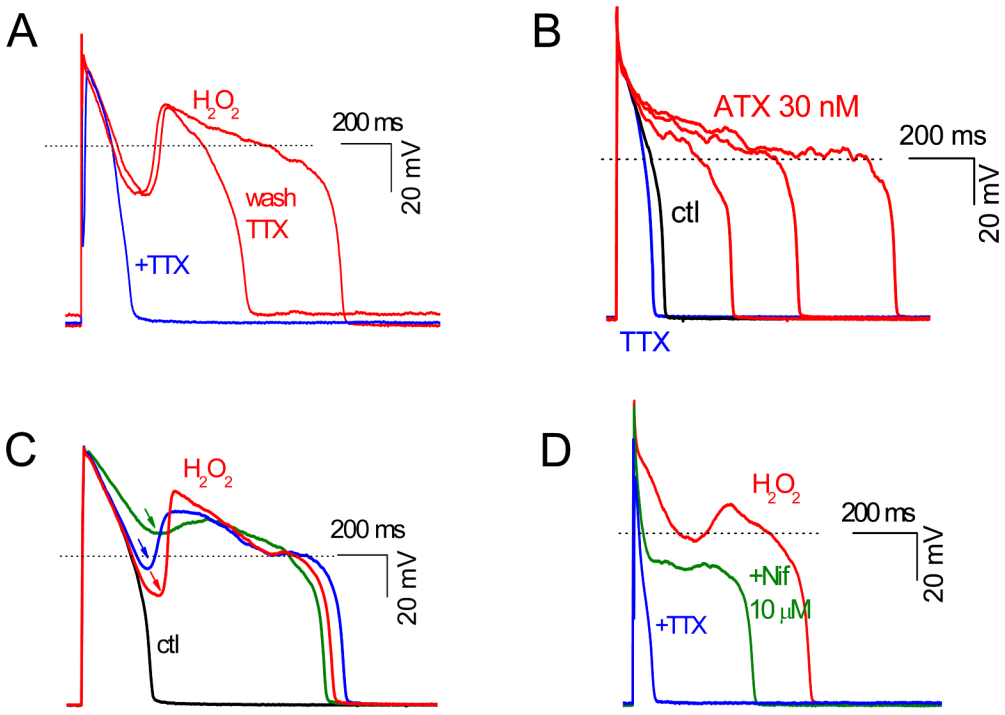

Fig. 7. Failure of KN-92, an inactive analog of KN-93, to prevent H_2O_2–induced EADs

A. Same protocol as in Fig. 6A, but with KN-92 initially in place of KN-93. KN-92 failed to prevent EADs during exposure to 1 mM H_2O_2, which were subsequently partially suppressed by KN-93. APs at points a (control), b (~ 2 min after KN-92), c (KN-92 + H_2O_2) and d (KN-93 + H_2O_2) are shown below. **B.** Same as A, but applying BAPTA-AM to suppress EADs after KN-92 + H_2O_2.